HHS Public Access

Author manuscript

J Mol Cell Cardiol. Author manuscript; available in PMC 2019 January 01.

Published in final edited form as:

J Mol Cell Cardiol. 2018 January ; 114: 199–210. doi:10.1016/j.yjmcc.2017.11.017.

Sorcin ablation plus β-adrenergic stimulation generate an arrhythmogenic substrate in mouse ventricular myocytes

Xi Chen[1,5,*], **Craig Weber**[2], **Emily T. Farrell**[3], **Francisco J. Alvarado**[1,5], **Yan-Ting Zhao**[1], **Ana M. Gómez**[4], and **Héctor H. Valdivia**[1,*]

[1]Center for Arrhythmia Research, Department of Internal Medicine, Division of Cardiovascular Medicine, University of Michigan, Ann Arbor, MI 48109, USA

[2]Department of Physiology, University of Arizona College of Medicine, Tucson, AR 85724, USA

[3]Department of Pediatrics, Division of Cardiology, University of Wisconsin, Madison, WI 53705, USA

[4]UMR-S 1180, Faculté de Pharmacie, Université Paris-Sud, 92296 Chatenay-Malabry, FRANCE

[5]Department of Molecular and Integrative Physiology, University of Michigan, Ann Arbor, MI 48109, USA

Abstract

Sorcin, a penta-EF hand Ca^{2+}-binding protein expressed in cardiomyocytes, is known to interact with ryanodine receptors and other Ca^{2+} regulatory proteins. To investigate sorcin's influence on cardiac excitation-contraction coupling and its role in the development of cardiac malfunctions, we generated a sorcin knockout (KO) mouse model. Sorcin KO mice presented ventricular arrhythmia and sudden death when challenged by acute stress induced by isoproterenol plus caffeine. Chronic stress, which was induced by transverse aortic constriction, significantly decreased the survival rate of sorcin KO mice. Under isoproterenol stimulation, spontaneous Ca^{2+} release events were frequently observed in sorcin KO cardiomyocytes. Sorcin KO hearts of adult, but not young mice developed overexpression of L-type Ca^{2+} channel and Na^{+}-Ca^{2+} exchanger, which enhanced I_{Ca} and I_{NCX}. Consequently, spontaneous Ca^{2+} release events in sorcin KO cardiomyocytes were more likely to induce arrhythmogenic delayed afterdepolarizations. Our study demonstrates sorcin deficiency may trigger cardiac ventricular arrhythmias due to Ca^{2+} disturbances, and evidences the critical role of sorcin in maintaining Ca^{2+} homeostasis, especially during the adrenergic response of the heart.

[*]To whom correspondence should be addressed: Héctor H. Valdivia, MD, PhD, or Xi Chen BS, PhD candidate, University of Michigan, 2800 Plymouth Rd., 26-235N, Ann Arbor, MI 48109, Phone: 734-647-4001, hvaldiv@umich.edu; xichenum@umich.edu.

DISCLOSURE

None

Keywords

sorcin; ryanodine receptors; sodium-calcium exchanger; L-type Ca^{2+} channel; ventricular myocytes; cardiac ventricular arrhythmias

1. INTRODUCTION

Sorcin (soluble resistance-related calcium-binding protein) is a 21.6 kDa protein that belongs to the penta-EF hand protein family.[1,2] The protein acquires its name because it was first found to be overexpressed in multidrug-resistant cells.[3–6] However, further studies find that sorcin has a broad expression in cardiomyocytes, neurons, pancreatic β-cells, and vascular smooth muscle,[7–10] clearly transcending its potential role in multi-drug resistance. The binding of Ca^{2+} to sorcin ($K_{d,Ca}$~1 μM) moves EF hand 1 and 3, leading to a ~33% increase of solvent-accessible surface areas. The exposure of hydrophobic residues enables sorcin to translocate from cytosol to cellular membranes and to reach its target proteins.[1,2,9,11,12] Immunostaining shows that in the presence of Ca^{2+}, sorcin localizes at z-lines close to the T-tubules of adult mouse cardiomyocytes, which enables it to regulate proteins involved in excitation-contraction coupling (e-c coupling).[12,13] One key target protein of sorcin is ryanodine receptor 2 (RyR2), the sarcoplasmic reticulum (SR) Ca^{2+} release channel responsible for providing most of the Ca^{2+} necessary for cardiac contraction.[7] In single channel recordings of RyR2, sorcin decreases RyR2 activity in a fast (onset of effect is less than ~15 ms),[12] reversible, and dose-dependent manner.[14] Sorcin can also stimulate SR/ER Ca^{2+} ATPase (SERCA) activity by increasing its sensitivity to Ca^{2+} and enhancing the V_{max} of its Ca^{2+} pumping rate.[15] and significantly increases the sarcolemmal Na^{+}-Ca^{2+} exchanger (NCX) in rabbit cardiomyocytes.[16,17] Lastly, sorcin's effect on the L-type Ca^{2+} channel (LTCC) is more complex: while Meyers et al. find that sorcin accelerates Ca^{2+}-dependent inactivation of I_{Ca} leading to decreased I_{Ca} integral, Fowler et al. report that sorcin stimulates voltage-dependent inactivation but slows Ca^{2+}-dependent inactivation.[13,18]

The above *in vitro* experiments, most of which are conducted using purified exogenous sorcin protein, illustrate sorcin's effects on its target proteins but fail to profile the integral role of sorcin on e-c coupling in intact cardiomyocytes and whole hearts. As sorcin not only regulates RyR2 channels, but also influences Ca^{2+} entry and SR Ca^{2+} load by interacting with LTCC, SERCA and NCX, it is difficult to predict sorcin's global effects in intact systems. Previous research attempted to answer this question by using sorcin-overexpressing animals or cardiomyocytes, however, this approach may not be optimal because the method, time, and concentration used to expose sorcin to target proteins are critical determinants of its function. Also, a high concentration of sorcin or its long-term exposure is shown to be detrimental for cell function.[13,16,19,20] Thus, an alternative model is desired to provide novel critical insight into the role of endogenous sorcin in e-c coupling and heart function.

We generated a sorcin knockout (sorcin KO) mouse by ablating the exon 3 of *Sri*, the only sorcin-encoding gene. The sorcin KO mouse shows impaired insulin release due to ER stress in pancreatic β-cells,[8] but the effects of sorcin ablation in cardiac cells have not been studied. The sorcin KO mice enabled us to study the role of sorcin on e-c coupling in intact

cardiomyocytes, and to model the sorcin loss-of-function mutations found in patients/models with heart diseases.[11] By subjecting the sorcin KO mice to acute and chronic stress, we could determine the consequences of sorcin ablation and dysfunction under periods of Ca^{2+} overload. We found that sorcin KO mice were born without apparent phenotype and propagated at the expected Mendelian ratios, but displayed significantly higher incidence of cardiac arrhythmias and sudden death when subjected to stress. Hearts of adult sorcin KO mice (6-month-old), but not young mice (1-month-old) developed NCX and LTCC overexpression, which enhanced I_{NCX} and I_{Ca} density. Further, in isolated sorcin KO cardiomyocytes, isoproterenol stimulation triggered high incidence of delayed afterdepolarizations (DADs) accompanied with synchronized Ca^{2+} waves. We report for the first time that sorcin ablation plus β-adrenergic stimulation generate an arrhythmogenic substrate in ventricular myocytes that may trigger lethal arrhythmias due to global Ca^{2+} disturbances.

2. MATERIALS AND METHODS

2.1 Generation of sorcin KO mice

Portions of the murine *Sri* were obtained by screening the 129SV CITB BAC library (Invitrogen Inc.). A DNA fragment of *Sri* exon 1, 2, 3, 4 was cloned into pBluescriptSK (Stratagene Inc.) that contained the MC1-HSV-TK cassette. To remove axon 3, which presents in both sorcin isoforms (accession no. NM_001080974.2 and NM_025618.3), a mini targeting vector containing a loxP-flanked exon 3 and a loxP-flanked phosphoglycerol kinase (PGK) promoter-driven NEO-pGHpA cassette was generated. The mini targeting vector was transformed into the recombination-competent DY380 bacteria cells that previously transformed pBluescript-*Sri*-MC1-HSV-TK. Recombinants integrated the loxP-flanked exon 3 and loxP-flanked pGK promoter-NEO-pGHpA cassettes were selected as targeting vectors. The homologous integration of the mini targeting cassette into pBluescript-*Sri*-MC1-HSV-TK was confirmed by DNA sequencing.

The targeting vector was electroporated into mouse 129S1/SvImJ ES cells. ES cells integrated the targeting vector were selected by growth on G18. Neo^r, $GANC^r$ clones were picked, expanded, and genomic DNA were isolated from each clone. Correctly targeted colonies, 1C4, 1D12, 1E1, 2B7, 2F5, 2H11, were identified by the appearance of a 2.6k-bp band by using the ^{32}P autoradiogram 5′ probe. One euploid clone, 1D12, was microinjected into the blastocyst to produce a chimeric founder. The male chimera was mated with 129S1/SvImJ female (F_0). The $FloxNeo^{-/+}$ mouse in F_1 generation was selected to mate with EIIa-Cre transgenic mice to excise Neo cassette as well as *Sri* exon 3 (F_2). Three primers: sorIn3Rev 5′-GAA GGC TGG CAT GGA GTG AAA GCA-3′, sorIn2For 5′-CTG ACC TCA GTC AAC CAG TAA GTA GG-3′, and Neo 5′-CGT TGG CTA CCC GTG ATA TT-3′ were used to determine genotyping of mice. The excision of *Sri* exon 3 as well as Neo cassette was confirmed by a 453-bp band in PCR, which included a 3′ loxP site, a remnant 168-bp insertion from the targeting vector and neighboring intron, while WT DNA containing exon 3 presented a 1070-bp band. The $Sri^{+/-}$ mice was backcrossed to 129S1/SvImJ mice for 10 generations to eliminate Cre recombinase. Finally two $Sri^{+/-}$ mice were crossed to get the $Sri^{-/-}$ mice.

All animal experiments were approved by the University of Michigan Institutional Animal Care and Use Committee

2.2 Western blot

Expression of RyR2, LTCC, NCX and SERCA were measured in 6-month and 1-month-old sorcin KO mice as described before.[21] Heart frozen in liquid nitrogen was pulverized by pestle, and homogenized in lysis buffer containing 0.9% NaCl, 10 mM Tris-HCl pH 6.8, 20 mM NaF, 2 μM leupeptin, 100 μM phenylmethylsulphonyl fluoride, 500 μM benzamidine, 100nM aprotinin at 4°C. The sample was centrifuged at 1000 ×g for 10 minutes, and the supernatant was collected. The protein concentration was measured by Bradford method. For Western blots, 50 μg of lysate suspended in Laemmlii buffer was separated by SDS-PAGE in 4–20% TGX or AnyKD precast gels (Bio-Rad). Proteins were transferred to PVDF membranes at 25V for 16–18h at 4°C. Then, membranes were blocked in PBS-T containing (mM) 3 KH_2PO_4, 10 Na_2HPO_4, 150 NaCl, pH 7.2–7.4, 0.1% Tween 20) plus 5% dried skim milk. Proteins were probed with the following primary antibodies: sorcin (1:2000 custom), SERCA (1:1000, ab2861, Abcam), NCX (1:200, ab6495, Abcam), Cav1.2 (1:200, ACC-003, Alomone), RyR2 (1:2000, MA3-925, ThermoFisher). After the membrane being washed three times by PBS-T, membranes were incubated with goat anti-mouse-HRP (1:1000, 31437, Thermo) or goat anti-rabbit-HRP (1:2000, 31463, Thermo). Protein-antibody reactions were detected by using SuperSignal Femto ECL reagent (Thermo), and imaged by the ChemiDoc MP apparatus (Bio-Rad). Band intensity was analyzed by the ImageLab software (Bio-Rad).

2.3 Confocal Ca^{2+} imaging

Ca^{2+} activities, including Ca^{2+} spark, field stimulation-stimulated Ca^{2+} transient, SR Ca^{2+} load, and RyR2-mediated diastolic Ca^{2+} leak, were recorded by the LSM510 Meta inverted confocal microscope (Carl Zeiss) with a 40×/1.2 N. A water immerse objective. Cardiomyocytes were incubated with 10μM Fluo-4 AM, a cell-penetrating Ca^{2+} indicator with Ca^{2+} binding affinity (K_d) of ~335 nM, at 37°C for 5min. Then cells were washed and kept in fresh bath solution. Binding to Ca^{2+}, Fluo-4 presents an increase in fluorescence, which is excited at the wavelength of 488nm and recorded at wavelength >505nm. Ca^{2+} images were collected by the one-direction line scan of the long axis of cell, at the speed of 3.072ms/line. For β-adrenergic stimulation, 300nM isoproterenol was applied in bath solution. Ca^{2+} sparks, RyR2-mediated diastolic Ca^{2+} leak, Ca^{2+} transients, SR Ca^{2+} load, SERCA rate and NCX rate were measured as described in data supplement. For simultaneous recording of action potential and Ca^{2+} transient, cardiomyocytes were dialyzed with 0.2mM fluo-4 pentapotassium salt via pipette solution. Ca^{2+} transients were recorded by the Olympus IX51 inverted microscopy system with a 40×oil immerse objective.

2.4 Patch clamp

Whole-cell patch clamp experiments were conducted by using an Axopatch 700B and a Digidata 1440A digitizer (Axon Instruments) at room temperature. $I_{Ca,}$ $I_{NCX,}$ Action potential and action potential-triggered Ca^{2+} transient were measured as described in data supplement.

2.5 Electrocardiographic (ECG) recording

Mice were anesthetized by 5% isoflurane inhalation vaporized in oxygen at a flow rate of 0.8–1 L/min, and maintained at anesthetized state by 1.5–2% isoflurane. Mice were placed in a supine position on a heating pad of 37 °C, and needle ECG electrodes were placed under skin to record leads I and II ECG. After 10 min of baseline ECG recording, acute stress will be induced by intraperitoneal injection of epinephrine 2 mg/kg + caffeine 120 mg/kg. ECG was analyzed as described before.[22] After recording, mice were sacrificed by cervical dislocation.

2.6 Statistics

All data are presented as mean±SEM. Student t test, rank-sum test, two-way repeated-measures ANOVA, Holm-Sidak test, χ^2 test, Kaplan-Meier test were carried when appropriate to determine statistical significance. $p < 0.05$ was considered statistically significant.

Detailed methods for ventricular cardiomyocytes isolation, Ca^{2+} imaging (Ca^{2+} sparks, Ca^{2+} transient, SR Ca^{2+} load, RyR-mediated diastolic Ca^{2+} leak, NCX rate, SERCA rate), patch clamp recording (I_{Ca}, I_{NCX}, action potential), echocardiographic recording, transverse aortic constriction, Langendorff perfusion, and histological staining are described in data supplement.

3. RESULTS

3.1 Generation of sorcin knockout mice

This is the first description of the generation of the sorcin KO mouse. Figure 1A shows the strategy used to generate the targeting vector and the resultant targeted allele. 820-bp from *Sri*, which include exon 3 and neighboring introns, were excised by Cre-Lox recombination. The knockout of exon 3 of *Sri* was confirmed by a 453-bp band in the PCR of sorcin KO tissues (included the 3′ *LoxP* site, a remnant 168-bp insertion from the targeting vector, and neighboring intron), instead of the 1070-bp band detected in WT samples (Fig. 1B). Western blot using a sorcin antibody[12] demonstrated complete absence of the 21.6 kDa sorcin band in sorcin KO hearts (Fig. 1C). Crossbreeding of sorcin heterozygous mice yielded offspring with the expected Mendelian ratios of WT (sorcin$^{+/+}$ 22%), heterozygous (sorcin$^{-/+}$ 52%) and homozygous (sorcin$^{-/-}$ 26%) mice (Fig. 1D). Vertical planes of hearts indicated no structural alterations in sorcin KO hearts compared with WT (Fig. 1E), and echocardiographic parameters were all normal in adult (5~7-month-old) sorcin KO hearts (Suppl. Fig. 1). Thus, sorcin KO mice at baseline display no overt cardiac structural or functional alterations.

3.2 Arrhythmias and sudden death in sorcin KO hearts and mice under acute or chronic stress

The absence of overt structural or functional alterations in the sorcin KO mice was surprising, given the prominent role of sorcin in modulating proteins of e-c coupling.[12,13] However, lifespan of non-manipulated, freely-fed sorcin KO mice was shorter than WT littermates (18-month survival rate: KO 70% vs. WT 92.5%, N=40 in each group; Kaplan-

Meier test $p<0.05$) (Fig. 2A), suggesting there were concealed risk factors in sorcin KO mice uncovered by increase of age. To assess whether sorcin KO mice were in a pseudo-equilibrium state, we subjected them to chronic and acute stress. We first conducted transverse aortic constriction (TAC) to induce chronic stress in mice. After surgery, the survival rate in sorcin KO mice was significantly lower than that of WT (KO 52% vs. WT 88% after 3 weeks, N=24 in each group, Kaplan Meier test $p<0.01$,) (Fig. 2B). The substantial difference in survival rate indicated that the fragility of sorcin KO mice was exacerbated by TAC. Since no structural remodeling and difference in heart function were observed in sorcin KO mice after TAC (Suppl. Fig. 1), we assessed whether cardiac arrhythmias were part of the underlying mechanisms leading to accelerated death. We conducted acute stress tests in anesthetized 6-month-old mice, by i.p. injection of Epinephrine 2 mg/kg + caffeine 120 mg/kg.[23] Continuous recording of ECG activity showed that, whereas the WT group had few arrhythmic events, five out of 6 sorcin KO mice presented higher incidence of premature ventricular contractions (PVCs), bidirectional ventricular tachycardia (BVT), and ventricular tachycardia (VT) within 5 min after injection (Fig. 2C–E). One third of sorcin KO mice, but no WT, experienced sudden cardiac arrest during recording (Fig. 2F). The duration of ventricular arrhythmia was significantly longer in sorcin KO mice (356±151s) than WT (16.6±6.9s, $p<0.05$) (Fig. 2G), and two sorcin KO mice presented BVT for longer than 1000s. In agreement with *in vivo* test, freshly explanted and Langendorff-perfused sorcin KO hearts, although without significant difference in their response to isoproterenol (300 nM)-induced left ventricular developed pressure (Suppl. Fig. 2C), systolic (maximum) dp/dt (Suppl. Fig. 2D) and diastolic (minimum) dp/dt (Suppl. Fig. 2E), displayed increased incidence of PVCs and bigeminy/trigeminy compared to WT hearts (Suppl. Fig. 2A–B, F–H). Young (1-month-old) sorcin KO mice also presented higher incidence of premature contractions, bigeminy, and bidirectional ventricular tachycardia than WT littermates (Suppl. Fig. 3A–C). The duration of ventricular arrhythmias, however, was not different between young sorcin KO (19.15±4.44s) and WT mice (16.41±5.78s) (Suppl. Fig. 3D). These results showed that sorcin KO mice, while apparently normal under basal conditions, are thrown into tachyarrhythmias under acute sympathetic stimulation and fare worse than WT when subjected to chronic stress. Therefore, the shorter lifespan and increased TAC mortality of global sorcin KO mice may be due to cardiac alterations.

3.3 Electrophysiological remodeling in adult sorcin KO cardiomyocytes

The increased vulnerability of sorcin KO mice to arrhythmias and death under stress was intriguing and warranted examination of underlying mechanisms. We first determined whether the loss of sorcin led to altered expression of other proteins involved in e-c coupling by using Western blots. NCX and LTCC (Cav1.2) were ~2.2-fold and 2.4-fold, respectively, increased in *adult* (6-month-old) sorcin KO hearts compared to WT, while the expression of SERCA and RyR2 was unaltered (Fig. 3A, B). Interestingly, young (1-month-old) sorcin KO hearts did not present overexpression of LTCC and NCX as adult hearts. Instead, the expression of NCX in young KO hearts was modestly lower than WT (Fig. 3C, D). No other changes were noted.

To assess whether the overexpression of NCX and LTCC in adult sorcin KO hearts had a functional correlation, we measured NCX (Fig. 4) and LTCC (Fig. 5) activities. NCX

activity was first determined from the rate of decay of the caffeine-induced Ca^{2+} transient ($K_{caffeine}$), defined as $1/\tau$ (where τ = the time constant of the decay phase). Adult sorcin KO cardiomyocytes had comparable $K_{caffeine}$ as WT under basal condition, but exhibited faster $K_{caffeine}$ under 300 nM isoproterenol stimulation, reflecting faster Ca^{2+} reuptake rate by NCX (Fig. 4A, B). To directly evaluate this parameter, we recorded NCX current (I_{NCX}) in patch-clamped cells, in which free $[Ca^{2+}]_i$ was set at ~210 nM by adding 6 mM Ca^{2+} and 10 mM ethylene glycol-bis(β-aminoethyl ether)-N,N,N′,N′-tetraacetic acid (EGTA) in the pipette solution. NCX current,generated by exchanging 3 Na^+ ions for 1 Ca^{2+} ion, was determined by subtracting the Ni^{2+}-sensitive currents (Fig. 4C).[16,17] NCX inward current is the forward-mode depolarizing current (Ca^{2+} out, Na^+ in) at membrane potential lower than −60 mV and turns to reverse-mode (Ca^{2+} in, Na^+ out) during depolarization. Adult sorcin KO and WT cardiomyocytes had comparable I_{NCX} under basal condition (Fig. 4D) but KO cardiomyocytes had significantly larger outward current (clamped at 50~80 mV) and inward current (clamped at −120~−80 mV) under isoproterenol stimulation (Fig. 4C, E). The increased $K_{caffeine}$ as well as I_{NCX} in sorcin KO cardiomyocytes suggested that although the stimulating effect of sorcin on NCX[16,17] was not present in sorcin KO cells, NCX activity was enhanced under isoproterenol stimulation. It is likely that the overexpression of NCX protein detected by Western blots allowed for a more robust $[Ca^{2+}]_i$ extrusion, resulting in enhanced NCX activity observed in isoproterenol-stimulated sorcin KO cardiomyocytes.

We then measured L-type Ca^{2+} current (I_{Ca}) of adult sorcin KO and WT cardiomyocytes. Sorcin KO cardiomyocytes presented modestly but statistically significant increased peak I_{Ca} compared to WT under basal condition (Two-way RM ANOVA $p<0.05$) (Fig. 5A). The robust stimulating effect of isoproterenol blurs most of the difference in peak I_{Ca}, although at −20 mV sorcin KO cardiomyocytes still displayed significantly higher I_{Ca} than WT (Holm-Sidak test $p<0.05$) (Fig. 5B). As ours and other groups' research have shown sorcin does not influence amplitude of I_{Ca},[12,13] the increased peak I_{Ca} in sorcin KO cardiomyocytes corresponded to LTCC overexpression.

Although I_{Ca} peak increased in adult sorcin KO cardiomyocytes under basal condition, the Ca^{2+}-dependent fast inactivation of I_{Ca} (τ_{fast}) significantly accelerated at the same time (Fig. 5C) so the total I_{Ca} (Σ_{ICa}) was not significantly changed. On the other hand, under isoproterenol stimulation, τ_{fast} of I_{Ca} in adult sorcin KO cardiomyocytes was slower than that of WT, which favors more Ca^{2+} entry during e-c coupling (Fig. 5D).

3.4 Ca^{2+} transients and SR Ca^{2+} load in adult sorcin KO cardiomyocytes

We previously showed that sorcin (3 μM) dialyzed into cardiomyocytes via pipette significantly decreased intracellular Ca^{2+} transient amplitude and e-c coupling gain,[12] underscoring sorcin as a potent inhibitor of I_{Ca}-triggered RyR2 activity. To investigate the effect of endogenous sorcin on I_{Ca}-triggered Ca^{2+} release during contraction, we measured Ca^{2+} transients by pacing Fluo-4 loaded cardiomyocytes at 1Hz for 20 s (Fig. 6A). During pacing, the Ca^{2+} transient amplitude gradually decreased until SR Ca^{2+} reached a steady level. We used the averaged peak value of the last 10 Ca^{2+} transients of a train of stimulation to represent the Ca^{2+} transient amplitude.

Mirroring the increased I_{Ca} amplitude in sorcin KO cardiomyocyte and sorcin's inhibitory effect on I_{Ca}-induced RyR2 activity, sorcin KO cardiomyocytes presented modest but statistically higher Ca^{2+} transient amplitude than WT under basal conditions, but the difference disappeared under isoproterenol stimulation, as higher diastolic Ca^{2+} leak in sorcin KO cardiomyocytes (see below) dampened Ca^{2+} release (Fig. 6B). The total SR Ca^{2+} load in resting cardiomyocyte, measured as caffeine-induced Ca^{2+} release after pacing, was not different between sorcin KO and WT cardiomyocytes (Fig. 6C). Sorcin KO cardiomyocytes presented slower Ca^{2+} pumping rate by SERCA under isoproterenol stimulation (Fig. 6D), which bodes well with previous results showing that sorcin stimulates SERCA function.[15]

3.5 Isoproterenol reveals increased Ca^{2+} leak in sorcin KO cardiomyocytes

We tested whether sorcin ablation leads to increased RyR2 activity by measuring Ca^{2+} sparks after pacing. After a 20-s train of field stimulation at 1Hz, both WT and sorcin KO cardiomyocytes had few Ca^{2+} sparks under basal conditions. Notably, however, sorcin KO cells exhibited higher frequency of Ca^{2+} sparks under isoproterenol stimulation (Fig. 7A, E). The spark amplitude, full duration at half maximum (FDHM), and half decay time were all significantly higher in sorcin KO cardiomyocytes (Fig. 7B, F–H). Since SR Ca^{2+} load of sorcin KO cardiomyocytes was not significantly changed (Fig. 6C), the result suggests increased SR Ca^{2+} cycling in KO cells, and RyR2 hyperactivity during diastole.

To ascertain more categorically whether RyR2 activity is increased in KO cells, we measured RyR2-mediated diastolic SR Ca^{2+} leak by an alternative method, as described by Shannon *et al.*[24] Cardiomyocytes were perfused in $0Na^{+}$-$0Ca^{2+}$ solution, which stopped Ca^{2+} exchange between extracellular and intracellular compartments as LTCC and NCX were blocked. Then, tetracaine (1mM) was perfused to block Ca^{2+} leak through RyR2. The fluorescence difference before and after tetracaine perfusion reflected diastolic Ca^{2+} leak (Fig. 7C, D). Sorcin KO cardiomyocytes had diastolic SR Ca^{2+} leak comparable to WT under basal condition but displayed higher diastolic SR Ca^{2+} leak under isoproterenol stimulation (Fig. 7C, D, I). The difference was maintained after the Ca^{2+} leak was normalized to the SR Ca^{2+} load.

3.6 Prolonged action potential duration and delayed afterdepolarizations in adult sorcin KO cardiomyocytes

Western blots and patch clamp recordings suggested electrophysiological remodeling of I_{Ca} and I_{NCX} in adult sorcin KO cardiomyocytes, which may play a key role in maintaining SR Ca^{2+} load and contractility in isoproterenol-stimulated sorcin KO cardiomyocytes. Although electrophysiological remodeling plays important compensatory effects, it may turn sorcin KO mice more susceptible to arrhythmias because: 1) The enhanced inward I_{NCX} during diastole can lead to membrane depolarization and further, may trigger arrhythmogenic DADs if fired by spontaneous Ca^{2+} release;[25] 2) both increased inward I_{Ca} and I_{NCX} may prolong AP repolarization and induce early afterdepolarizations (EADs).[26,27] We recorded action potentials (APs) and Ca^{2+} transients simultaneously[28] to investigate if the electrophysiological remodeling described above brings about arrhythmogenic events in sorcin KO cardiomyocytes. Under basal condition, while most sorcin KO cardiomyocytes

had normal APs and Ca^{2+} transients (Suppl. Fig. 4A, B), 4 out of 12 sorcin KO cells presented random EADs, which were accompanied by spontaneous Ca^{2+} release events between pacing (Supp. Fig. 4C). In the aggregate, however, EAD frequency was not statistically different between sorcin KO and WT cardiomyocytes (p=0.128) (Suppl. Fig. 4D). With the appearance of EADs, 6 out of 12 KO cells had APD_{90} longer than 300 ms (Suppl. Fig. 4E). APD at 70, 75, 80, and 90 percent of repolarization were significantly increased in sorcin KO cells compared to WT (p<0.001, WT n=11, KO n=12), although APD variability was large (Suppl. Fig. 4E, 4F). In summary, most of sorcin KO cardiomyocytes presented normal APs and Ca^{2+} transients under basal conditions. Although some sorcin KO cardiomyocytes presented EADs and extremely long APD, the incidence did not reach statistical significance and so the KO mice did not present ventricular arrhythmias nor long Q-T interval at baseline. Nonetheless, the phenomenon might be a sign of disturbed Ca^{2+} homeostasis in sorcin KO cardiomyocytes.

Under isoproterenol stimulation, sorcin KO cardiomyocytes had significantly higher frequency of spontaneous Ca^{2+} waves than WT (Fig. 8A–C). Seventy-eight percentage (47/60) of spontaneous Ca^{2+} waves in sorcin KO cardiomyocytes led to membrane depolarizations (i.e., DADs) that were of sufficient amplitude to reach threshold for I_{Na} activation, thus triggering full-blown APs (Fig. 8B insert, D). By contrast, only 35% (6/17) of spontaneous Ca^{2+} waves developed into triggered activities in WT cardiomyocytes, while the rest only led to mild (<20mV) membrane depolarization (Fig. 8A, D). As sorcin KO cardiomyocytes had higher incidence of spontaneous Ca^{2+} waves, and their Ca^{2+} waves led to APs more readily, the frequency of triggered activities in sorcin KO cardiomyocytes was dramatically higher than WT (Fig. 8E). Sorcin KO cardiomyocytes also presented significantly longer APDs at 70, 80, and 90 percent of repolarization under isoproterenol stimulation (Fig. 8F, G). DADs and EADs were fully prevented in KO cells dialyzed with10 mM fast Ca^{2+} chelator 1,2-bis(*o*-aminophenoxy)ethane-*N*,*N*,*N*′,*N*′-tetraacetic acid (BAPTA), which completely quenched Ca^{2+}-induced Ca^{2+} release during e-c coupling (Suppl. Fig. 5A, C). However, 37.5% of KO cells still presented DADs with coordinated "Ca^{2+} spikes" when dialyzed with 10 mM Ca^{2+} chelator EGTA, whose Ca^{2+} binding rate was ~100 times slower than BAPTA (Suppl. Fig. 5B, C). Both BAPTA and EGTA significantly decreased action potential duration of sorcin KO cardiomyocytes (Suppl. Fig. 5D). The results suggested that $[Ca^{2+}]_i$ is necessary to trigger electrical alterations in the sarcolemma of sorcin KO cardiomyocytes.

4. DISCUSSION

Sorcin, a 21.6-kDa Ca^{2+} binding protein originally discovered in multi-drug resistance cells, is also expressed in ventricular cardiomyocytes of mammalian species, including humans.[1,29] This is a basic observation that compels a fundamental question: *what does sorcin do in cardiac cells?* We previously found that the majority of sorcin is localized in bands of high intensity running along the width of the cardiomyocyte, interspaced at about ~1.7 μm, and overlapping with RyR2 located in *z*-lines.[12,13] Thus, a great portion of sorcin appears localized in the dyadic junction, where crucial steps of e-c coupling occur. Also, using single RyR2 channels or isolated ventricular cells, we found that sorcin rapidly binds to RyR2 and directly inhibits single channel activity, translocates from soluble to membrane-bound

protein targets in a Ca^{2+}-dependent manner, and attenuates Ca^{2+} sparks and Ca^{2+} transients in saponin-permeabilized cardiomyocytes.[12] These and other findings affirmed a role for sorcin in modulation of Ca^{2+} release by RyR2s, but its integral role in Ca^{2+} homeostasis and e-c coupling of the heart remained unclear. Here, we generated a mouse line with genetic ablation of *Sri,* the gene encoding for sorcin in humans and animal. These mice were born without apparent phenotype, propagated at the expected Mendelian ratio, and most survived into adulthood (Fig. 1). However, hearts from young (1-month-old) sorcin KO mice, although showing no apparent electrical remodeling, were nonetheless thrown into transient tachyarrhythmia episodes upon β-adrenergic stimulation (Supp. Fig. 3), indicating that sorcin absence *per se* predisposes mice to arrhythmias. As sorcin KO mice developed into adulthood, an increase in LTCC and NCX expression (Fig. 3) and activity (Figs. 4, 5) suggests cardiac contractions become increasingly dependent on sarcolemma Ca^{2+} entry and extrusion. Thus, the prolonged absence of sorcin plus its resultant electrical remodeling appear to lead the adult sorcin KO mice to a precarious condition, because a) their survival rate was lower than WT, even under resting condition (Fig. 2A), b) aortic banding that was tolerated by WT mice caused significantly more attrition in sorcin KO mice (Fig. 2B), c) stress tests promptly induced long-lasting tachyarrhythmias and sudden cardiac arrest (Figs. 2C–G, Suppl. Fig. 2). All these results, therefore, support the hypothesis that sorcin is a stabilizing component of the e-c coupling machinery of the heart, independent of or in addition to other roles that it may play in other cells.

4.1 Sorcin KO phenotype and resemblance to CPVT

Sorcin ablation brings about significant alterations in Ca^{2+} homeostasis of ventricular myocytes, and this becomes more apparent under β-adrenergic stimulation: isolated cardiomyocytes stimulated with isoproterenol display Ca^{2+} sparks, Ca^{2+} oscillations, aftercontractions, and DAD-elicited triggered activity (Figs. 7, 8). Bidirectional ventricular tachycardia, characteristic of Ca^{2+}-overloaded cells and a hallmark of CPVT,[30,31] is also present in sorcin KO mice (Fig. 2, Suppl. Fig. 3). The general features of the sorcin KO phenotype are thus strikingly similar to those of catecholaminergic polymorphic ventricular tachycardia (CPVT), which is typically associated with RyR2 hyperactivity. In both cases, a cardiac phenotype is “silent” functionally and structurally and goes unnoticed until sympathetic stimulation triggers catastrophic Ca^{2+} release and life-threatening arrhythmias (Figs. 2, 7, 8).[30] We postulate, therefore, that RyR2 channels are among the most prominent molecular targets of sorcin in ventricular cardiomyocytes and the most affected by its absence.

4.2 Amplification of sorcin effect by sympathetic stimulation

During normal β-adrenergic stimulation, RyR2s are especially active due to increased I_{Ca} and higher SR Ca^{2+} load. Ca^{2+} release from a cluster of RyR2s into the dyadic nanospace could theoretically increase local [Ca^{2+}] up to ~100 μM,[32,33] which is sufficient to translocate sorcin to SR membrane targets. By decreasing RyR2 activity, sorcin conceivably attenuates Ca^{2+}-induced Ca^{2+} release and helps prevent Ca^{2+}-triggered membrane depolarization. On the other hand, sorcin has been shown to be PKA-phosphorylated at residue S178,[2,14,15] and others[15] and we (unpublished data) have shown that phosphorylation facilitates translocation of sorcin from cytosolic to membrane

compartments. Therefore, the high [Ca^{2+}] in the dyadic space and sorcin phosphorylation during β-adrenergic stimulation amplify sorcin's regulatory effect on RyR2, its key target.

4.3 Hypothesis for an integrated role of sorcin in e-c coupling

While initial experiments to elucidate sorcin's role in the heart demonstrated that sorcin inhibits Ca^{2+} release by RyR2 channels, equally compelling are the findings that sorcin increases NCX activity,[16,17] accelerates LTCC inactivation,[13,34] and stimulates SERCA Ca^{2+} uptake.[15] Therefore, sorcin forms macromolecular complexes with at least four key players of e-c coupling. By summing the individual effects exerted by sorcin on the above-mentioned Ca^{2+} transporters, it seems obvious that the unified role for sorcin in cardiac cells is to restrict I_{Ca}-triggered RyR2 activity and avoid Ca^{2+} accumulation in cytosolic compartments. However, what is not immediately obvious is that such an integrated effect is not possible in the long run, because it would eventually deplete cardiac cells of Ca^{2+} by restricting Ca^{2+} entry and release and stimulating Ca^{2+} extrusion. In a delimited and finely regulated system such as a ventricular cell, inward and outward Ca^{2+} fluxes must be equal, and in this zero-sum game, small disturbances are rapidly counteracted, lest profound alterations in electrical excitability, e-c coupling and signal conduction ensue.[35] Therefore, a process that mitigates adrenergic-induced Ca^{2+} buildup is necessary, and we propose that sorcin is an integral part of such a process. Sorcin's Ca^{2+} removal role may be especially active during β-adrenergic stimulation of the heart, right after cardiac cells have transitioned to Ca^{2+} overload due to a rapid surge of plasmalemmal Ca^{2+} entry. It is during this time window that Ca^{2+} fluxes are briefly unbalanced because the β adrenergic-induced Ca^{2+} overload, while maximizing contractions, promotes also the generation of DADs (by spontaneous Ca^{2+} release) and EADs (by prolonging APD). If removal of adrenergic-induced Ca^{2+} buildup by sorcin is indeed necessary, then sorcin KO mice should develop arrhythmias mainly during β-adrenergic stimulation, or under stress. In favor of this hypothesis, others and we found that adrenergic stimulation of ventricular cells increases translocation of sorcin from cytosolic to membrane-bound targets[15] and that sorcin KO hearts and living mice are readily thrown into tachyarrhythmias under sympathetic simulation. Thus, the overall hypothesis that emerges from this and previous studies is that sorcin "sweeps" cytosolic compartments from excess Ca^{2+} during periods of Ca^{2+} overload.

4.4 General model to explain arrhythmias in young and adult sorcin KO mice

From the above, we propose a *model* that integrates the major mechanisms governing the induction of arrhythmias in young and adult sorcin KO mice. First, the model must consider fundamental differences in e-c coupling between immature (neonatal and young mice) and adult ventricular cells, with the former relying more on external Ca^{2+} entry due to incompletely formed t-tubules and dyads,[36] while the latter obtaining from the SR (by Ca^{2+}-induced Ca^{2+} release) most of the Ca^{2+} needed for contractions.[37] Second, the model must also consider data showing increased LTCC and NCX density in adult, but not in young, sorcin KO cardiomyocytes, as observed here (Fig. 3). In both cases, however, β-adrenergic stimulation increases contractility by increasing Ca^{2+} cycling. Hence, in the absence of sorcin, a modulator that normally decreases Ca^{2+} entry, promotes Ca^{2+} extrusion, stimulates SR Ca^{2+} reuptake, and decreases SR Ca^{2+} fluxes, the most plausible mechanism to induce ventricular arrhythmias in the *immature* hearts is one in which the adrenergically-stimulated

cytosolic Ca^{2+} surges generate an inward depolarizing current of sufficient magnitude to bring membrane potential to threshold, generating DADs and subsequent triggered activity. This mechanism would be akin to that postulated to occur in CPVT[30] and does not require electrical remodeling (normal expression of e-c coupling proteins). On the other hand, abnormal expression of e-c coupling proteins in the *mature* sorcin KO hearts suggests gradual adaptation of the e-c coupling machinery to the absence of sorcin: the increased SR Ca^{2+} leak and decreased SERCA pumping may eventually prompt sorcin KO cardiomyocytes to become more dependent on external Ca^{2+} to activate contractions and reload the SR, hence, sorcin KO cells must increase their pool and/or their activity of LTCC (Figs. 3, 5). The increased Ca^{2+} influx (Ca^{2+} in, Na^{+} out) through overexpressed NCX (Figs. 3, 4) during the upstroke of action potential also makes contribution to maintaining SR Ca^{2+} release. Since a larger Ca^{2+} entry and SR Ca^{2+} leak cannot be sustained without a comparable Ca^{2+} extrusion mechanism, the 2.2-fold increase in the density of sarcolemmal NCX (Figs. 3, 4), who works in forward mode (Ca^{2+} out, Na^{+} in) during diastole, represents such concomitant Ca^{2+} extrusion mechanism. In this hypothetical scheme, adult sorcin-null ventricular cells appear to tilt the balance between sarcolemmal and SR Ca^{2+} fluxes to maintain a pseudo-equilibrium that is stable under basal conditions but favors arrhythmias under adrenergic stimulation.

4.5 Limitations of our study

Our general hypothesis above, while viable and accommodating of our major observations here, requires further testing and experimentation that go beyond the scope of this study. First, as it happens with most transgenic animals, ablation of a single gene seldom results in “clean” knockout of the target protein, because such targeted gene and protein interact with a variety of (known and unknown) partners that constitute an indivisible functional network. In the case of the sorcin KO, we performed a *targeted* analysis of what we considered the most relevant sorcin-interacting proteins and found alterations in some, but not all, binding partners. Wider changes in protein expression would not be surprising, and they may even force key revisions of our hypothesis. Second, sorcin is encoded by a single gene (*Sri*) and expressed in several tissues, therefore, it is possible that the cardiac arrhythmias or the decreased lifespan of sorcin KO mice reported here may have extra-cardiac origins. For example, we previously reported that the absence of sorcin in pancreatic β-cells triggers ER stress,[8] and it is possible that the resultant glucose intolerance may have impacted cardiac function.[38] Even though our experiments using isolated, Langendorff-perfused hearts indicate that cardiac arrhythmias are present in the absence of autonomic nerve system or hormonal input, we cannot completely discard this possibility. Lastly, the majority of sorcin localizes in immunocytochemical experiments to the dyadic space and near RyR2,[12,13] but a small portion (~18%) does not. The first study describing expression of sorcin in cardiac cells[7] found anti-sorcin reactivity in mitochondria. The potential impact of mitochondria dysfunction to the cardiac arrhythmias described here, if any, requires an in-depth study of its own.

4.6 Summary

In summary, data here and published studies make it increasingly evident that sorcin modulates e-c coupling in the heart, at the very least through its well-established effect on

RyR2 channels, but also through newly-found molecular targets. Although our general hypothesis may require further testing, data obtained here with the sorcin KO mouse does lay some solid foundations to postulate a unified role for sorcin in cardiac cells: sorcin is a Ca^{2+}-dependent molecular switch that is activated during cytosolic Ca^{2+} surges, especially during β-adrenergic stimulation and, by binding to at least four key e-c coupling proteins, it removes Ca^{2+} from cytosolic compartments and avoids Ca^{2+}-dependent arrhythmias.

Supplementary Material

Refer to Web version on PubMed Central for supplementary material.

Acknowledgments

We are grateful to Patricia Powers, Biotechnology Center of the University of Wisconsin, for technical support in the generation of the sorcin KO mice and to Timothy Hacker (University of Wisconsin) for echocardiographic and TAC experiments.

SOURCES OF FUNDING

This work was supported by the National Institutes of Health [grant numbers R01-HL055438, R01-HL120108, and R01-HL134344 (to HHV)]; and the French National Research Agency [grant number ANR-13-BSV1-0023-01 (to AMG)].

GLOSSARY

AP	action potential
BAPTA	1,2-bis(o-aminophenoxy)ethane-N,N,N′,N′-tetraacetic acid
BVT	bidirectional ventricular tachycardia
CPVT	catecholaminergic polymorphic ventricular tachycardia
DAD	delayed afterdepolarization
EAD	early afterdepolarization
e-c coupling	excitation-contraction coupling
EGTA	ethylene glycol-bis(β-aminoethyl ether)-N,N,N′,N′-tetraacetic acid
FDHM	full duration at half maximum
LTCC	L-type Ca^{2+} channel
NCX	Na^{+}-Ca^{2+} exchanger
PVC	premature ventricular contraction
RyR2	ryanodine receptor type 2
SERCA	SR/ER Ca^{2+} ATPase

Sorcin KO	sorcin knockout
SR	sarcoplasmic reticulum
TAC	transverse aortic constriction
VT	ventricular tachycardia

References

1. Ilari A, Fiorillo A, Poser E, Lalioti VS, Sundell GN, Ivarsson Y, Genovese I, Colotti G. Structural basis of Sorcin-mediated calcium-dependent signal transduction. Sci Rep. 2015; 5:16828. [PubMed: 26577048]
2. Ilari A, Johnson KA, Nastopoulos V, Verzili D, Zamparelli C, Colotti G, Tsernoglou D, Chiancone E. The crystal structure of the sorcin calcium binding domain provides a model of Ca2+-dependent processes in the full-length protein. J Mol Biol. 2002; 317:447–458. [PubMed: 11922676]
3. Van der Bliek AM, Baas F, Van der Velde-Koerts T, Biedler JL, Meyers MB, Ozols RF, Hamilton TC, Joenje H, Borst P. Genes amplified and overexpressed in human multidrug-resistant cell lines. Cancer Res. 1988; 48:5927–5932. [PubMed: 2901906]
4. Deng L, Su T, Leng A, Zhang X, Xu M, Yan L, Gu H, Zhang G. Upregulation of soluble resistance-related calcium-binding protein (sorcin) in gastric cancer. Med Oncol. 2010; 27:1102–1108. [PubMed: 19885748]
5. Maddalena F, Laudiero G, Piscazzi A, Secondo A, Scorziello A, Lombardi V, Matassa DS, Fersini A, Neri V, Esposito F, Landriscina M. Sorcin induces a drug-resistant phenotype in human colorectal cancer by modulating Ca(2+) homeostasis. Cancer Res. 2011; 71:7659–7669. [PubMed: 22052463]
6. Dabaghi M, Rahgozar S, Moshtaghian J, Moafi A, Abedi M, Pourabutaleb E. Overexpression of SORCIN is a Prognostic Biomarker for Multidrug-Resistant Pediatric Acute Lymphoblastic Leukemia and Correlates with Upregulated MDR1/P-gp. Genet Test Mol Biomarkers. 2016; 20:516–521. [PubMed: 27382961]
7. Meyers MB, Pickel VM, Sheu SS, Sharma VK, Scotto KW, Fishman GI. Association of sorcin with the cardiac ryanodine receptor. J Biol Chem. 1995; 270:26411–26418. [PubMed: 7592856]
8. Marmugi A, Parnis J, Chen X, Carmichael L, Hardy J, Mannan N, Marchetti P, Piemonti L, Bosco D, Johnson P, Shapiro JA, Cruciani-Guglielmacci C, Magnan C, Ibberson M, Thorens B, Valdivia HH, Rutter GA, Leclerc I. Sorcin Links Pancreatic beta-Cell Lipotoxicity to ER Ca2+ Stores. Diabetes. 2016; 65:1009–1021. [PubMed: 26822088]
9. Rueda A, Song M, Toro L, Stefani E, Valdivia HH. Sorcin modulation of Ca2+ sparks in rat vascular smooth muscle cells. J Physiol. 2006; 576:887–901. [PubMed: 16931553]
10. Gracy KN, Clarke CL, Meyers MB, Pickel VM. N-methyl-D-aspartate receptor 1 in the caudate-putamen nucleus: ultrastructural localization and co-expression with sorcin, a 22,000 mol. wt calcium binding protein. Neuroscience. 1999; 90:107–117. [PubMed: 10188938]
11. Franceschini S, Ilari A, Verzili D, Zamparelli C, Antaramian A, Rueda A, Valdivia HH, Chiancone E, Colotti G. Molecular basis for the impaired function of the natural F112L sorcin mutant: X-ray crystal structure, calcium affinity, and interaction with annexin VII and the ryanodine receptor. FASEB J. 2008; 22:295–306. [PubMed: 17699613]
12. Farrell EF, Antaramian A, Rueda A, Gomez AM, Valdivia HH. Sorcin inhibits calcium release and modulates excitation-contraction coupling in the heart. J Biol Chem. 2003; 278:34660–34666. [PubMed: 12824171]
13. Meyers MB, Fischer A, Sun YJ, Lopes CM, Rohacs T, Nakamura TY, Zhou YY, Lee PC, Altschuld RA, McCune SA, Coetzee WA, Fishman GI. Sorcin regulates excitation-contraction coupling in the heart. J Biol Chem. 2003; 278:28865–28871. [PubMed: 12754254]
14. Lokuta AJ, Meyers MB, Sander PR, Fishman GI, Valdivia HH. Modulation of cardiac ryanodine receptors by sorcin. J Biol Chem. 1997; 272:25333–25338. [PubMed: 9312152]

15. Matsumoto T, Hisamatsu Y, Ohkusa T, Inoue N, Sato T, Suzuki S, Ikeda Y, Matsuzaki M. Sorcin interacts with sarcoplasmic reticulum Ca(2+)-ATPase and modulates excitation-contraction coupling in the heart. Basic Res Cardiol. 2005; 100:250–262. [PubMed: 15754088]
16. Seidler T, Miller SL, Loughrey CM, Kania A, Burow A, Kettlewell S, Teucher N, Wagner S, Kogler H, Meyers MB, Hasenfuss G, Smith GL. Effects of adenovirus-mediated sorcin overexpression on excitation-contraction coupling in isolated rabbit cardiomyocytes. Circ Res. 2003; 93:132–139. [PubMed: 12805242]
17. Zamparelli C, Macquaide N, Colotti G, Verzili D, Seidler T, Smith GL, Chiancone E. Activation of the cardiac Na(+)-Ca(2+) exchanger by sorcin via the interaction of the respective Ca(2+)-binding domains. J Mol Cell Cardiol. 2010; 49:132–141. [PubMed: 20298697]
18. Fowler MR, Colotti G, Chiancone E, Higuchi Y, Seidler T, Smith GL. Complex modulation of L-type Ca(2+) current inactivation by sorcin in isolated rabbit cardiomyocytes. Pflugers Arch. 2009; 457:1049–1060. [PubMed: 18830620]
19. Suarez J, Belke DD, Gloss B, Dieterle T, McDonough PM, Kim YK, Brunton LL, Dillmann WH. In vivo adenoviral transfer of sorcin reverses cardiac contractile abnormalities of diabetic cardiomyopathy. Am J Physiol Heart Circ Physiol. 2004; 286:H68–75. [PubMed: 12958030]
20. Frank KF, Bolck B, Ding Z, Krause D, Hattebuhr N, Malik A, Brixius K, Hajjar RJ, Schrader J, Schwinger RH. Overexpression of sorcin enhances cardiac contractility in vivo and in vitro. J Mol Cell Cardiol. 2005; 38:607–615. [PubMed: 15808837]
21. Alvarado FJ, Chen X, Valdivia HH. Ablation of the cardiac ryanodine receptor phospho-site Ser2808 does not alter the adrenergic response or the progression to heart failure in mice. Elimination of the genetic background as critical variable. J Mol Cell Cardiol. 2017; 103:40–47. [PubMed: 28065668]
22. Loaiza R, Benkusky NA, Powers PP, Hacker T, Noujaim S, Ackerman MJ, Jalife J, Valdivia HH. Heterogeneity of ryanodine receptor dysfunction in a mouse model of catecholaminergic polymorphic ventricular tachycardia. Circ Res. 2013; 112:298–308. [PubMed: 23152493]
23. Cerrone M, Colombi B, Santoro M, di Barletta MR, Scelsi M, Villani L, Napolitano C, Priori SG. Bidirectional ventricular tachycardia and fibrillation elicited in a knock-in mouse model carrier of a mutation in the cardiac ryanodine receptor. Circ Res. 2005; 96:e77–82. [PubMed: 15890976]
24. Shannon TR. Quantitative Assessment of the SR Ca2+ Leak-Load Relationship. Circulation Research. 2002; 91:594–600. [PubMed: 12364387]
25. Schlotthauer K, Bers DM. Sarcoplasmic reticulum Ca(2+) release causes myocyte depolarization. Underlying mechanism and threshold for triggered action potentials. Circ Res. 2000; 87:774–780. [PubMed: 11055981]
26. Weiss JN, Garfinkel A, Karagueuzian HS, Chen PS, Qu Z. Early afterdepolarizations and cardiac arrhythmias. Heart Rhythm. 2010; 7:1891–1899. [PubMed: 20868774]
27. Madhvani RV, Angelini M, Xie Y, Pantazis A, Suriany S, Borgstrom NP, Garfinkel A, Qu Z, Weiss JN, Olcese R. Targeting the late component of the cardiac L-type Ca2+ current to suppress early afterdepolarizations. J Gen Physiol. 2015; 145:395–404. [PubMed: 25918358]
28. Zhao YT, Valdivia CR, Gurrola GB, Powers PP, Willis BC, Moss RL, Jalife J, Valdivia HH. Arrhythmogenesis in a catecholaminergic polymorphic ventricular tachycardia mutation that depresses ryanodine receptor function. Proc Natl Acad Sci U S A. 2015; 112:E1669–1677. [PubMed: 25775566]
29. Suarez J, McDonough PM, Scott BT, Suarez-Ramirez A, Wang H, Fricovsky ES, Dillmann WH. Sorcin modulates mitochondrial Ca(2+) handling and reduces apoptosis in neonatal rat cardiac myocytes. Am J Physiol Cell Physiol. 2013; 304:C248–256. [PubMed: 23151801]
30. Priori SG, Chen SR. Inherited dysfunction of sarcoplasmic reticulum Ca2+ handling and arrhythmogenesis. Circ Res. 2011; 108:871–883. [PubMed: 21454795]
31. Priori SG, Napolitano C, Memmi M, Colombi B, Drago F, Gasparini M, DeSimone L, Coltorti F, Bloise R, Keegan R, Cruz Filho FE, Vignati G, Benatar A, DeLogu A. Clinical and molecular characterization of patients with catecholaminergic polymorphic ventricular tachycardia. Circulation. 2002; 106:69–74. [PubMed: 12093772]

32. Cannell MB, Kong CH, Imtiaz MS, Laver DR. Control of sarcoplasmic reticulum Ca2+ release by stochastic RyR gating within a 3D model of the cardiac dyad and importance of induction decay for CICR termination. Biophys J. 2013; 104:2149–2159. [PubMed: 23708355]

33. Zhao YT, Valdivia HH. Ca2+ nanosparks: shining light on the dyadic cleft but missing the intensity of its signal. Circ Res. 2014; 114:396–398. [PubMed: 24481836]

34. Meyers MB, Puri TS, Chien AJ, Gao T, Hsu PH, Hosey MM, Fishman GI. Sorcin associates with the pore-forming subunit of voltage-dependent L-type Ca2+ channels. J Biol Chem. 1998; 273:18930–18935. [PubMed: 9668070]

35. Ter Keurs HE, Boyden PA. Calcium and arrhythmogenesis. Physiol Rev. 2007; 87:457–506. [PubMed: 17429038]

36. Snopko RM, Ramos-Franco J, Di Maio A, Karko KL, Manley C, Piedras-Renteria E, Mejia-Alvarez R. Ca2+ sparks and cellular distribution of ryanodine receptors in developing cardiomyocytes from rat. J Mol Cell Cardiol. 2008; 44:1032–1044. [PubMed: 18468619]

37. Bers DM. Cardiac excitation-contraction coupling. Nature. 2002; 415:198–205. [PubMed: 11805843]

38. Giles TD, Sander GE. Diabetes mellitus and heart failure: basic mechanisms, clinical features, and therapeutic considerations. Cardiol Clin. 2004; 22:553–568. [PubMed: 15501623]

Highlights

- Sorcin KO mice present arrhythmias and sudden death under acute or chronic stress.
- Adult sorcin KO cardiomyocytes develop electrophysiological remodeling.
- Isoproterenol reveals spontaneous Ca^{2+} release events in sorcin KO cardiomyocytes.
- Sorcin KO cardiomyocytes present high incidence of triggered activities.

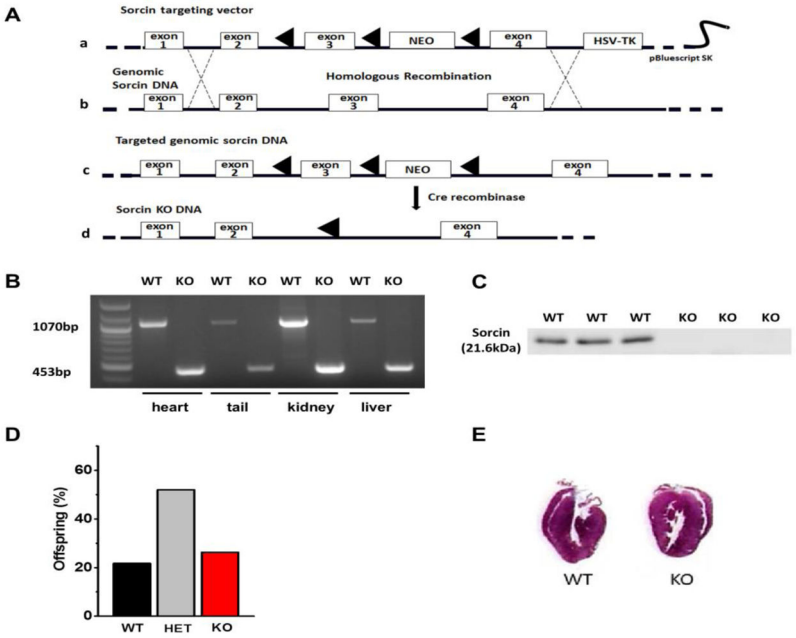

Figure 1. Generation of sorcin KO mice

(A) Strategy for the generation of sorcin KO mice by homologous recombination. **a.** The sorcin targeting vector containing *LoxP*-flanked exon 3 of *SRI*, *LoxP*-flanked Neo-cassette and the HSV-TK cassette; **b.** WT *SRI* containing seven exons (four exons are shown in graph); **c.** Homologous recombination between the endogenous *SRI* and sorcin targeting vector results in a DNA carrying *LoxP*-flanked *SRI* exon 3 and Neo-cassette. **d.** Sorcin KO DNA is created by the Cre-excision of *SRI* exon 3 and Neo-cassette. (B) PCR confirmation of WT and sorcin KO mice. Instead of the 1070-bp band seen in WT, a 453-bp band is detected in sorcin KO allele. (C) Western blot with sorcin antibody confirms the presence of sorcin in 3 WT hearts (first three bands) and its absence in 3 sorcin KO mice. (D) Crossbreeding of sorcin heterozygous mice yields the expected proportion of WT (sorcin $^{+/+}$), heterozygous (sorcin$^{-/+}$) and homozygous knockout (sorcin$^{-/-}$) mice. (E) Vertical planes of hearts indicate no structural alterations in sorcin KO heart compared with WT.

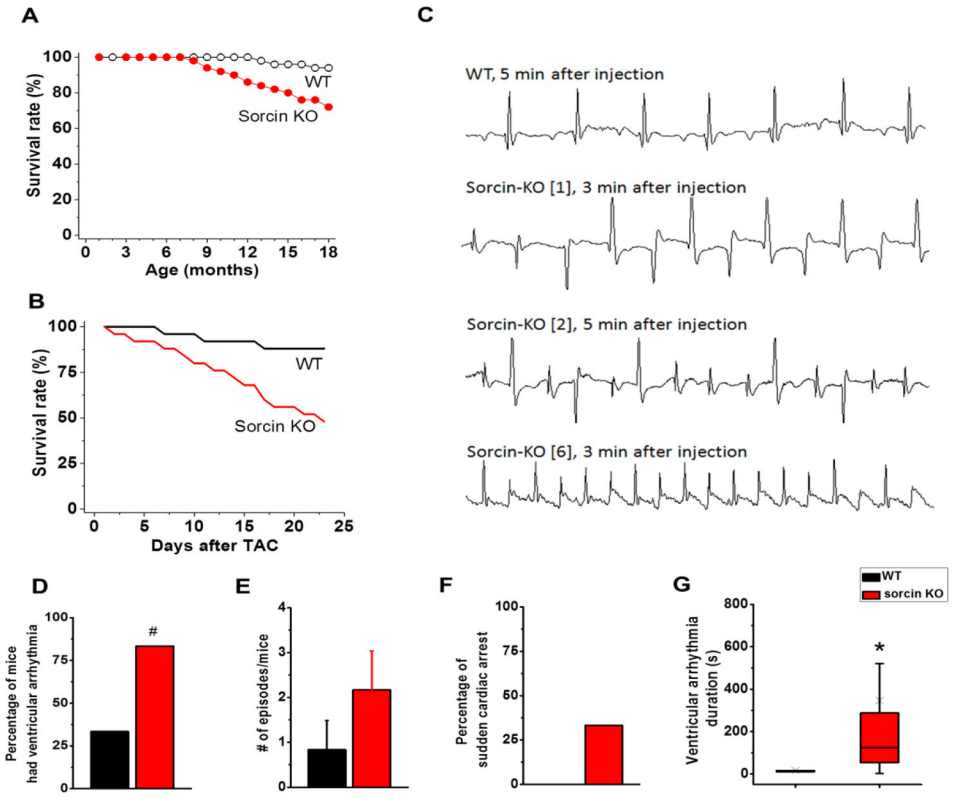

Figure 2. Life span, ECG and survival rate of mice

(A) Long-term follow up of lifespan of sorcin KO and WT mice. N=40/group. Kaplan-Meier test $p<0.05$. (B) Survival rate of 6-month-old mice after the conduction of transverse aortic constriction (TAC) N=24/group. Kaplan-Meier test $p<0.01$. (C) ECG recordings of 6-month-old anesthetized mice after the administration of epinephrine (2 mg/kg) + caffeine (120 mg/kg). First trace: representative ECG of a WT mouse after 5 min of injection; second trace: bidirectional ventricular tachycardia (BVT) in a sorcin KO mouse after 3 min of injection; third trace: premature ventricular contractions (PVCs) in a sorcin KO mouse after 5 min of injection; fourth trace: ventricular tachycardia (VT) in a sorcin KO mouse after 3 min of injection. Each trace is 1s recording. (D) Percentage of mice that had ventricular arrhythmia after injection. (E) Number of ventricular arrhythmia episodes in WT and sorcin KO mice, per arrhythmia cocktail challenge. (F) Percentage of mice that presented sudden cardiac arrest after injection. (G) Duration of arrhythmias in WT and sorcin KO mice. N=6 in each group. ×, average value; *, $p<0.05$ vs. WT, #, $p=0.051$ vs. WT.

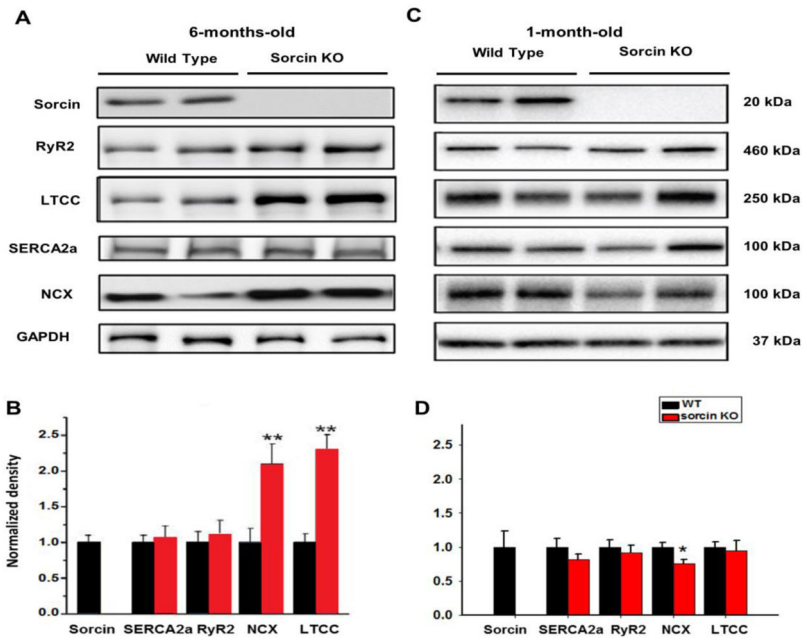

Figure 3. Expression of Ca^{2+} regulatory proteins

(A–B) Representative Western blots (A) and quantification (B) for sorcin, SERCA2a, RyR2, NCX, and LTCC expression in 6-month-old WT and sorcin KO hearts. (C–D) Representative Western blots (C) and quantification (D) for protein expression in 1-month-old WT and sorcin KO hearts. N=5 in each group. *, $p<0.05$ vs. WT; ** $p<0.01$ vs. WT.

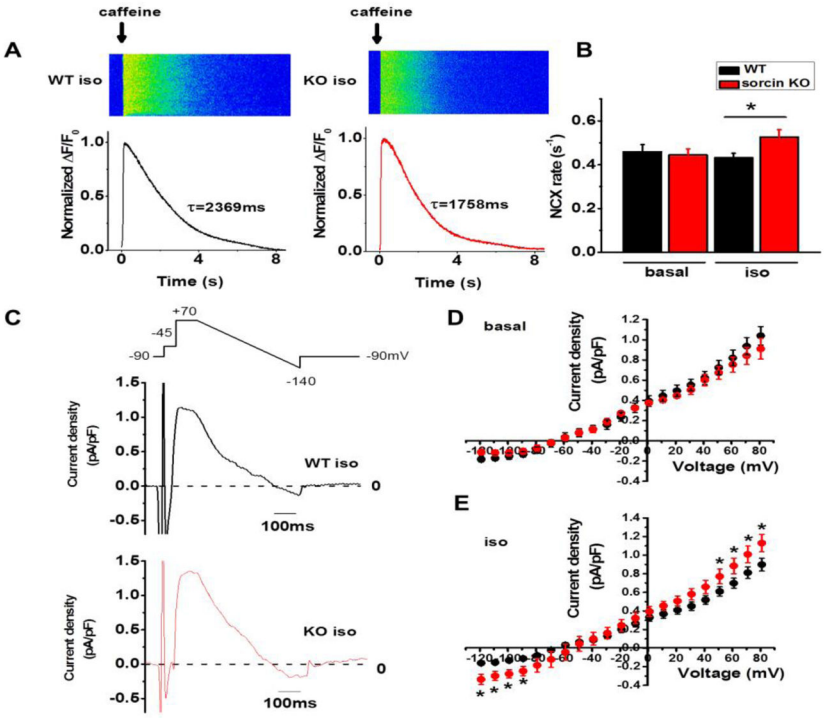

Figure 4. NCX activity

(A) Representative Ca^{2+} imaging and plot of caffeine-induced Ca^{2+} transient in WT and sorcin KO cardiomyocytes. WT $\tau_{caf\ f}$= 2369 ms, KO τ_{caff}= 1758 ms. (B) NCX rate (K_{NCX}). WT-basal n=10, KO-basal n=9; WT-iso n=12, KO-iso n=13. (C) Protocol for recording I_{NCX} and representative I_{NCX} of WT and sorcin KO cardiomyocytes under isoproterenol stimulation. (D) I–V curve of I_{NCX} under basal condition. WT-basal n=9, KO-basal n=8 (E) I–V curve of I_{NCX} under isoproterenol stimulation. WT-iso n=9, KO-iso n=9. *, p<0.05 vs. WT.

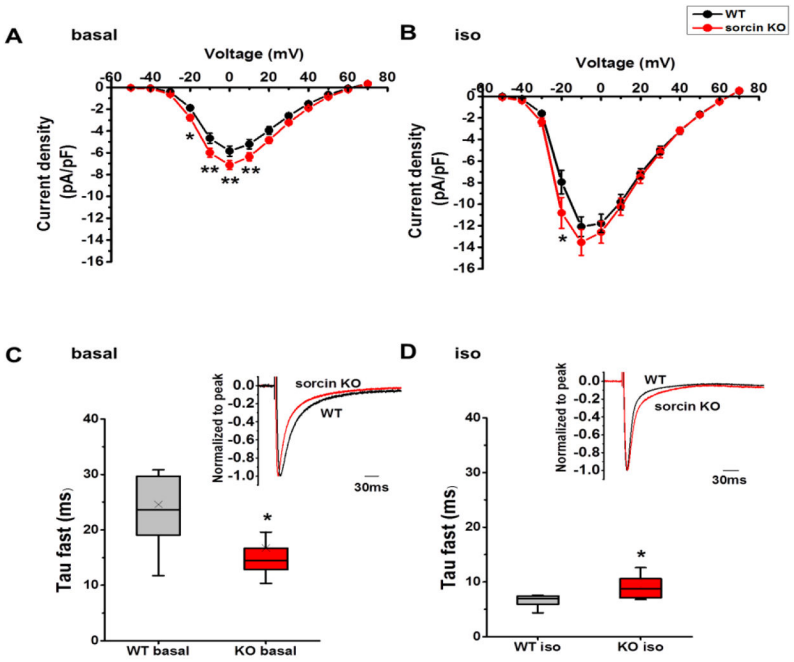

Figure 5. L-type Ca^{2+} current

(A–B) I–V curve of I_{Ca} under basal condition (A), and under isoproterenol stimulation (B). (C) τ_{fast} of I_{Ca} inactivation at 0 mV under basal condition. Insert: representative curves of I_{Ca} at 0 mV under basal condition. (D) τ_{fast} of I_{Ca} inactivation at −10 mV under isoproterenol stimulation. Insert: representative curves of I_{Ca} at −10 mV under isoproterenol stimulation. WT-basal n=11, KO-basal n=14, WT-iso n=10, KO-iso n=10. *, $p<0.05$ vs. WT.

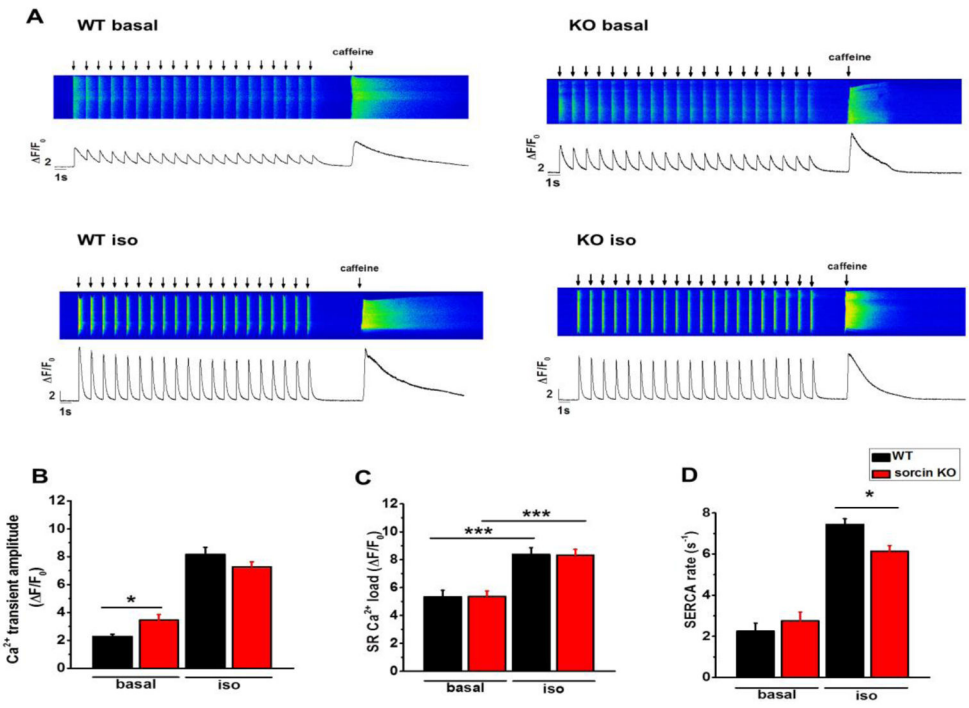

Figure 6. Intracellular Ca^{2+} transients

(A) Representative recordings of Ca^{2+} transients and SR Ca^{2+} load of WT and sorcin KO cardiomyocytes under basal condition and isoproterenol stimulation. Cardiomyocytes were paced 20 times and 10 mM caffeine was perfused to the cell after pacing to measure SR Ca^{2+} load. (B–D) Ca^{2+} transient amplitude (B), SR Ca^{2+} load (C), and SERCA rate (D) of WT and sorcin KO cardiomyocytes under basal condition and isoproterenol stimulation. WT-basal n=13, KO-basal n=14, WT-iso n=13, KO-iso n=16. *, $p<0.05$ vs. WT; ***, $p<0.001$ vs. WT.

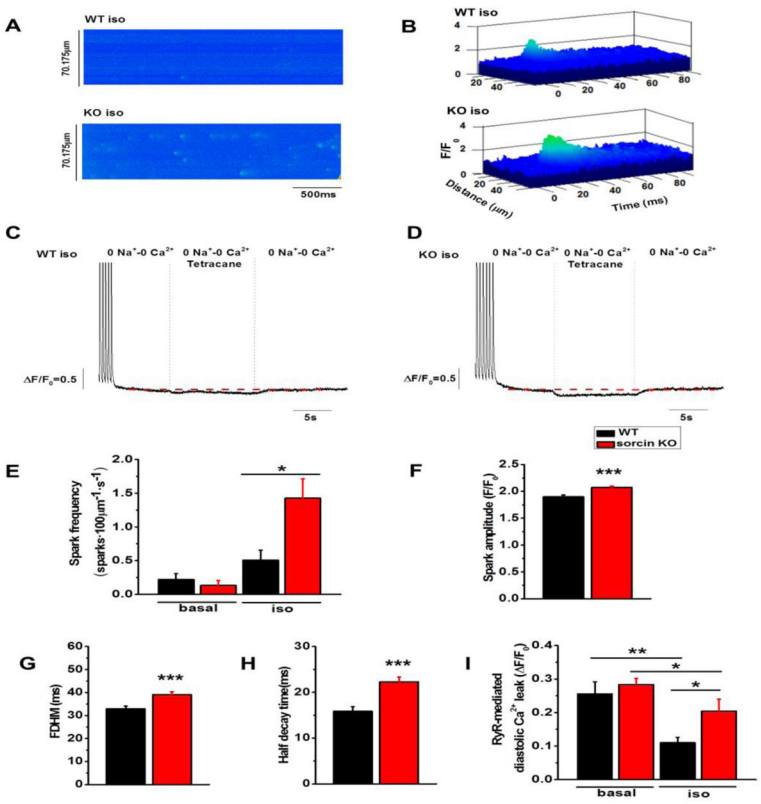

Figure 7. Ca^{2+} sparks and leak in cardiomyocytes

(A) Ca^{2+} sparks of WT and sorcin KO cardiomyocytes under isoproterenol stimulation. Sparks were measured after 20 times of 1Hz pacing. (B) 3D plots of representative Ca^{2+} sparks of WT and sorcin KO cardiomyocytes. (C–D) Representative plots of RyR2-mediated SR Ca^{2+} leak of WT (C) and sorcin KO (D) cardiomyocytes under isoproterenol stimulation. Cardiomyocytes were perfused in $0Na^{+}$-$0Ca^{2+}$ solution. Then, tetracaine (1 mM) was added to block Ca^{2+} leak through RyR2. After 10s, tetracaine was washed out by $0Na^{+}$-$0Ca^{2+}$ solution. The fluorescence difference before and after tetracaine application (marked by red dashed line) reflects RyR-mediated diastolic Ca^{2+} leak. (E–H) Ca^{2+} spark frequency of cardiomyocytes under basal condition and isoproterenol stimulation (E), Ca^{2+} sparks amplitude (F), full duration at half maximum (FDHM) (G), and half decay time (H) under isoproterenol stimulation. WT-basal n=16, KO-basal n=16, WT-iso n=16, KO-iso n=32 cells. (I) RyR2-mediated diastolic SR Ca^{2+} leak under basal condition and isoproterenol stimulation. WT-basal n=11, KO-basal n=15; WT-iso n=12, KO-iso n=12 cells. *, $p<0.05$ vs. WT or sorcin KO; **, $p<0.01$ vs. WT under basal condition; ***, $p<0.001$ vs. WT under isoproterenol stimulation.

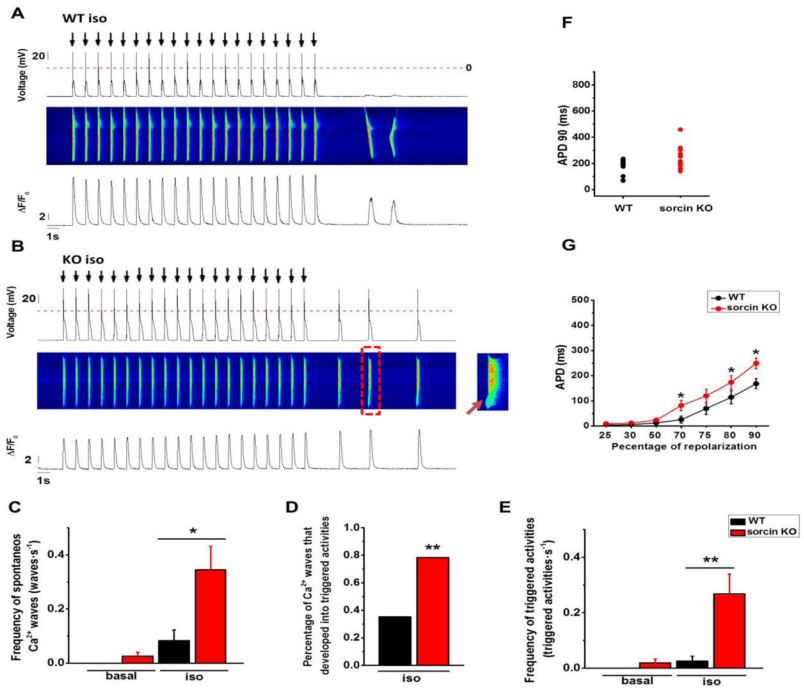

Figure 8. Action potential and Ca^{2+} transients under isoproterenol stimulation

(A) Representative WT cardiomyocyte that presented spontaneous Ca^{2+} release events but not triggered activity under isoproterenol stimulation. Upper panel: action potential; arrows indicate the time when the electrical stimulus was applied; middle panel: fluorescent recording of Ca^{2+} transient; under panel: line plot of Ca^{2+} transient. (B) Representative sorcin KO cardiomyocyte that presented triggered activities under isoproterenol stimulation. Insert at right: expanded image of the spontaneous Ca^{2+} wave in the red frame, showing how a localized Ca^{2+} release (arrow) ignited a full Ca^{2+} transient and triggered activity. (C) Frequency of spontaneous Ca^{2+} waves in quiescent state. (D) Percentage of spontaneous Ca^{2+} waves that developed into triggered activity under isoproterenol stimulation: 3 out of 14 and 47 out of 60 spontaneous Ca^{2+} waves in WT and sorcin KO cardiomyocytes, respectively, developed into triggered activities. (E) Frequency of triggered activities in quiescent state. (F) Scatter plot of under isoproterenol stimulation. Each dot represents a different cell. (G) APD at APD_{90} indicated percent of repolarization under isoproterenol stimulation. WT-basal n=11, WT-iso n=12, KO basal n=10, KO-iso n=14 cells. *, $p<0.05$ vs. WT; **, $p<0.01$ vs. WT.